European Journal of Nuclear Medicine and Molecular Imaging (2021) 48:3493–3501
https://doi.org/10.1007/s00259-021-05343-x

ORIGINAL ARTICLE

Value of [^{68}Ga]Ga-FAPI-04 imaging in the diagnosis of renal fibrosis

Yue Zhou[1,2,3] · Xin Yang[4,5] · Huipan Liu[1,2,3] · Wenbin Luo[6] · Hanxiang Liu[1,2,3] · Taiyong Lv[1,2,3] · Junzheng Wang[1,2,3] · Jianhua Qin[4,5] · Santao Ou[4,5] · Yue Chen[1,2,3]

Received: 16 January 2021 / Accepted: 25 March 2021 / Published online: 7 April 2021

Abstract

Purpose Renal fibrosis is a pathological state in the progression of chronic kidney disease. Early detection and treatment are vital to prolonging patient survival. Renal puncture examination is the gold standard for renal fibrosis, but it has several limitations. This study aims to evaluate the diagnostic performance of a novel PET radiotracer, [^{68}Ga]Ga-fibroblast activation protein inhibitor (FAPI)-04, which specifically images fibroblast activation protein (FAP) expression for renal fibrosis.

Methods All patients underwent renal puncture before receiving [^{68}Ga]Ga-FAPI-04 PET/CT imaging. They then underwent [^{68}Ga]Ga-FAPI-04 PET/CT and immunochemistry examinations. The data obtained were analyzed.

Results The [^{68}Ga]Ga-FAPI-04 PET/CT examination results demonstrated that almost all patients (12/13) exhibited increased radiotracer uptake. The maximum standardized uptake value (SUVmax) in patients with mild, moderate, and severe fibrosis was 3.92 ± 1.50, 5.98 ± 1.6, and 7.67 ± 2.23, respectively.

Conclusion Compared with renal puncture examination, non-invasive imaging of FAP expression through [^{68}Ga]Ga-FAPI-04 PET/CT quickly demonstrates bilateral kidney conditions with high sensitivity. [^{68}Ga]Ga-FAPI-04 PET/CT can facilitate the evaluation of disease progression, diagnosis, and the development of a treatment plan.

Keywords Renal fibrosis · [^{68}Ga]Ga-FAPI · PET/CT · Renal puncture

Introduction

Renal fibrosis refers to the pathological changes caused by the deposition of extracellular matrix in the kidney, including glomerulosclerosis, renal interstitial fibrosis, and arteriosclerosis [1, 2]. It does not refer to a specific disease but rather to a pathological state in the progression of almost all chronic kidney diseases (CKDs), which often indicates an irreversible decline in renal function. Renal fibrosis is closely related to patient prognosis. As renal fibrosis progresses, functional nephrons gradually decrease, eventually progressing to end-stage renal disease (ESRD) [3, 4]. Due to a lack of reliable, easy assessment methods, it is difficult to precisely determine renal fibrosis prevalence. However, given the 10.8%

Yue Zhou and Xin Yang contributed equally to this work.

This article is part of the Topical Collection on Radiopharmacy

✉ Yue Chen
chenyue5523@126.com

Santao Ou
ousantao@163.com

[1] Department of Nuclear Medicine, The Affiliated Hospital of Southwest Medical University, No 25 TaiPing St, Jiangyang District, Luzhou, Sichuan 646000, People's Republic of China

[2] Academician (Expert) Workstation of Sichuan Province, The Affiliated Hospital of Southwest Medical University, Luzhou, Sichuan, People's Republic of China 646000

[3] Nuclear Medicine and Molecular Imaging Key Laboratory of Sichuan Province, The Affiliated Hospital of Southwest Medical University, Luzhou, Sichuan, People's Republic of China 646000

[4] Department of Nephrology, The Affiliated Hospital of Southwest Medical University, No 25 TaiPing St, Jiangyang District. No 25 TaiPing St, Jiangyang District, Luzhou, Sichuan 646000, People's Republic of China

[5] Sichuan Clinical Research Center for Nephropathy, The Affiliated Hospital of Southwest Medical University, Luzhou, Sichuan, People's Republic of China 646000

[6] Department of Cardiology, Daping Hospital of The Third Military Medical University, Chongqing, People's Republic of China 400042

prevalence of CKD, it can be inferred that many patients have renal fibrosis [5].

There is a growing body of renal fibrosis research. At present, many factors are believed to affect renal fibrosis, including myofibroblasts, many cytokines, such as TGF-β, transcription factors, macrophages, and autophagy. Partial epithelial-mesenchymal transition (pMET) deepens our understanding of renal fibrosis [6–11]. An accurate assessment of renal fibrosis is important to patients' diagnosis, treatment, and efficacy judgment.

Fibroblast activation protein (FAP) is a member of the cell surface dipeptidyl peptidase (DPP) family of serine proteases. FAP is involved in inflammatory and fibrotic tissues [12–16]. Kidney damage can cause inflammatory cell infiltration and the myofibroblasts a large number of extracellular matrix components produced by, which in turn lead to renal fibrosis [17–20]. The radiolabeled FAP inhibitor [^{68}Ga]Ga-FAPI-04 was developed as a radiotracer for PET/CT imaging. At present, its clinical value for renal fibrosis has not been systematically studied. This research aims to improve the detection rate of renal fibrosis through non-invasive imaging technology and facilitate clinical diagnosis and treatment.

Patients, materials, and methods

Patients

A total of 13 patients who had undergone renal puncture at the Affiliated Hospital of Southwest Medical University between January and October of 2020 were enrolled in the study. Hematoxylin-eosin (HE) and periodic acid-Schiff (PAS) staining showed that the patients' kidneys had varying degrees of renal fibrosis. The study excluded all patients with general health conditions affecting cardiopulmonary function/mental status and allergies to alcohol. This study was approved by the Ethics Committee of the First Affiliated Hospital of Southwest Medical University and followed the 1964 Helsinki Declaration and its subsequent amendments to the ethical standards. All patients signed written informed consent forms. [^{68}Ga]Ga-FAPI-04 was provided based on compassionate use. All patients underwent PET/CT examinations, and immunochemical examinations were performed on the kidney tissues collected before patients were enrolled in the study (see Table 1 for patients' information).

Table 1 Detailed demographics and extent of disease of patients

Patient no.	Age/gender	Type of nephropathy	Extent of disease			Immunochemical examination		SUVmax of kidney	SUVmean of liver	TBR
			Degree of renal fibrosis (HE & PAS)	GFR (mL/min)	Scr (umol/L)	Glomerular fibrosis	Renal interstitial fibrosis			
1	66/F	Membranous nephropathy	II	58.2	88.6	0	2+	3.91	0.547	7.15
2	58/M	Membranoproliferative glomerulonephritis	III	8.3	604.6	1+	1+	5.71	0.569	10.03
3	56/F	Minimal change glomerulonephritis	I	87.7	67.2	0	1+	4.4	0.72	6.11
4	25/M	Mesangial proliferative glomerulonephritis	I	100.4	92.5	0	1+	4.5	0.521	8.64
5	47/M	Mesangial proliferative glomerulonephritis	I	24.4	262.6	1+	1+	4.3	0.478	8.99
6	18/F	Mesangial proliferative glomerulonephritis	III	11.9	642.4	0	2+	7.2	0.545	13.21
7	35/F	Mesangial proliferative glomerulonephritis	I	73.5	50.7	0	0	5.1	0.56	9.11
8	30/M	Crescentic glomerulonephritis	II	29.3	249	2+	0	7.3	0.892	8.18
9	30/F	Mesangial proliferative glomerulonephritis	I	115.3	81.9	0	0	1.3	0.522	2.49
10	25/M	Mesangial proliferative glomerulonephritis	II	58.8	143.9	0	2+	7.6	0.707	10.75
11	69/M	Membranoproliferative glomerulonephritis	III	31.5	148.8	0	1+	10.1	0.842	11.99
12	34/M	Mesangial Proliferative glomerulonephritis	II	35.7	206.6	0	2+	4.5	0.585	7.69
13	53/M	Membranoproliferative glomerulonephritis	II	64.5	113.3	1+	1+	6.6	0.825	8.003

The average age of the patients was 42.0 ± 17.0 (18–69 years). All patients showed pathological findings (HE and PAS staining) of renal fibrosis. Five patients had mild fibrosis, five had moderate fibrosis, and three had severe fibrosis. The evaluation parameters (including glomerulosclerosis, renal tubular atrophy, interstitial inflammation, and fibrosis) corresponded to the three grades I, II, and III, respectively, equivalent to affected proportions of <25%, 25–50%, and > 50%.

We retrospectively analyzed nine patients who underwent [^{68}Ga]Ga-FAPI-04 examination in the Department of Nuclear Medicine of the Affiliated Hospital of Southwest Medical University whose kidneys were not detected with abnormal radiotracer uptake as a normal control group.

Preparation of [^{68}Ga]Ga-FAPI-04

We purchased the precursor FAPI-04 from MCE (MedChemExpress, USA) with a purity grade of 98% and a mass of 872.91. FAPI-04 radiolabeling was performed according to the following protocol: 50 μg of FAPI-04 was dissolved in 1 mL of sodium acetate solution (0.25 M) and added 4 mL ^{68}Ga-solution (1.7 GBq) to a pH of 3.3–3.6. The reaction was heated at 80 °C for 10 min and the product was purified by using a Sep-pak ^{18}C column. It was then eluted with 1 mL of 50% ethanol and 4 mL of saline. Quality control was performed by radio-HPLC on an ^{18}C reverse phase column with a gradient elution of either H_2O with 0.1% TFA (solvent A) or CH_3CN with 0.1% TFA (solvent B). The mobile phase conditions were 0–50 min: 10–90% B, 1 mL/min. The radiochemical purity was over 98%.

Imaging and image analysis

Imaging was performed after the patient was in the Department of Nephrology, Affiliated Hospital of Southwest Medical University. Each patient provided a detailed medical history and underwent a physical examination before imaging. The intravenous radiotracer dose was 1.85–2.59 MBq/kg, and imaging was performed 50–60 min after radiotracer injection. All patients were required to urinate as much as possible for imaging preparations, which reduces the influence of the residual radiotracer in the renal pelvis and calyces. Some patients with poor renal function (GFR < 60 mL/min, urine volume < 1000 mL/24 h) were given diuretics (Furosemide, 0.57 mg/kg). The scope of the whole-body inspection was from the base of the skull to the base of the thigh, using five to six beds (3 min/bed). The matrix was 128 × 128, the PET layer thickness was 3 mm, and all PET images were reconstructed iteratively. All of the above inspection procedures were communicated to patients before obtaining their written informed consent.

The [^{68}Ga]Ga-FAPI-04 PET/CT image interpretation was based on visual and semi-directional analysis and was evaluated by two experienced nuclear medicine doctors. The mean standardized uptake value (SUVmean) of a round sphere with a diameter of 2 cm was selected from the liver as the activity background, and the SUVmax of the renal parenchyma was divided by this SUVmean to calculate target-to-background ratio (TBR). VOIs were located in the kidney parenchyma with increased radiotracer uptake [21], and the renal pelvis and calyces were avoided. The ROI diameter used by the kidney was 1 cm. Nuclear medicine and nephrology physicians checked the patient's general condition (mental state/blood pressure/heart-rate/body temperature) until 120 min after radiotracer injection and were required to report any abnormalities.

Immunochemistry

The kidney tissue was stained with an antibody against fibroblast activation protein-α (FAPα), treated with formalin, and then embedded in paraffin. All kidney tissues were obtained from the archives of the Department of Pathology, Affiliated Hospital of Southwest Medical University. The immunohistochemical image was evaluated by the scoring system adopted by Henry et al., in which kidney tissue is evaluated as 0 (no FAP immunostaining), 1+ (< 10% of stromal cells showing positive FAP staining), 2+ (10–50% of stromal cells showing positive FAP staining), and 3+ (> 50% of stromal cells showing positive FAP staining).

Statistical analysis

SPSS software (version 26.0; IBM, Armonk, NY) was used for statistical evaluation, and Graphpad8.0 was used for graphing. Measurement data were expressed as mean ± standard deviation. The Kruskal-Wallis nonparametric rank-sum test was used to compare the different degrees of renal fibrosis between groups. The Mann-Whitney *U* test was used to compare between sexes. $^{*}P < 0.05$ represents a comparison of the control group; $\#P < 0.05$ represents a comparison of the treatment group.

Results

Diagnostic performance of [^{68}Ga]Ga-FAPI-04 PET/CT in primary tumors

In this study, significant radiotracer uptake was detected in most patients (12/13). As the patients' HE and PAS staining showed the degree of renal fibrosis gradually increasing, patients' SUVmax, serum creatinine (Scr), and TBR gradually increased and their glomerular filtration rate (GFR) gradually

decreased. Patient indicators for different grades of renal fibrosis were compared by mean ± standard deviation. The renal SUVmax of healthy individuals (2.35 ± 0.55) was statistically significantly lower than that of patients with renal fibrosis grade II (5.98 ± 1.67) and III (7.67 ± 2.23) ($P < 0.05$). Meanwhile, the TBR of healthy individuals (3.30 ± 0.92) was statistically significantly lower than that of patients with renal fibrosis grade I (7.07 ± 2.84), II (8.35 ± 1.40), and III (11.74 ± 1.60) ($P < 0.05$). The GFR of patients with renal fibrosis grade I (86.26 ± 23.58) was statistically significantly higher than that of patients with renal fibrosis grade III (17.23 ± 12.49) ($P < 0.05$). However, the difference between patients in other groups was not statistically significant ($P > 0.05$). Figures 1, 2, 3, and 4 show some patient examination images, and Tables 2 and 3 and Fig. 5 show the study's statistical results.

Immunochemistry

Through immunohistochemical staining of antibodies specific for FAPα, FAP expression in renal interstitial cells was found in 10 patients (76.9%) and FAP expression in glomerular cells was found in four patients (Table 4) (30.7%). Figures 1, 2, 3, and 4 (g, h) show examples of FAP expression in renal fibrosis detected by immunochemistry.

Incidental findings

A diffusely increased radiotracer uptake (SUVmax = 11.7) was found in the breast of one young female patient, which may have been related to the patient's dense glands or changing hormone levels [22, 23]. Two patients' bilateral erector spinae also had increased radiotracer uptake. After questioning the two patients, we determined that they were employed in agriculture and as a bus driver, which may have damaged their erector spinae. They were diagnosed with erector spinae strain.

Table 2 Summary of patient characteristics

Description of patients (n=13)	13
Age, mean ± SD (range)	42.0±17.0 (18–69 years)
Gender (M:F)	8:05
TBR (positive)	12 (92%)
SUVmax (positive)	12 (92%)
GFR (<75 mL/min)	10 (77%)
SCR (>97umol/L)	8 (62%)
Degree of renal fibrosis(HE)	
I	5 (38%)
II	5 (38%)
III	3 (23%)

Table 3 Comparison of indicators between the three degrees of renal fibrosis

Indicators	TBR	SUVmax	GFR (mL/min)	SCR (umol/L)
Degree of renal fibrosis				
I	7.07±2.84	3.92±1.50	86.26±23.58	110.98±86.21
II	8.35±1.40	5.98±1.68	49.30±15.70	160.28±66.39
III	11.74±1.60	7.67±2.23	17.23±12.49	465.27±274.72
P value	0.038	0.039	0.016	0.016

Adverse events

All patients tolerated the [^{68}Ga]Ga-FAPI-04 PET/CT examination well. There were no signs of drug-related pharmacological effects or physiological reactions. All patients' vital signs (blood pressure/heart-rate/body temperature) were kept within the normal range before, during, and after the examination. No patients reported any abnormalities.

Comparison with other non-invasive imaging examinations and suitability

At present, the main non-invasive imaging examinations for renal fibrosis are magnetic resonance, ultrasound, and enhanced CT. There is a lack of consensus regarding MRI's detection of renal fibrosis due to conflicting reports, which affects reliability [24]. Ultrasound examination of renal fibrosis has low specificity and is easily affected by factors such as the doctor's subjective judgment, examination preparation, and abdominal effusion [25, 26]. Enhanced CT may damage the patient's kidneys due to the use of contrast agents and intravenous hydration [27]. [^{68}Ga]Ga-FAPI-04 PET/CT may be suitable for patients with renal fibrosis, including abnormal blood coagulation function, renal parenchymal atrophy, acute renal fibrosis, and negative puncture tests.

Discussion

To date, no serological indicators have been found that specifically reflect the degree of renal fibrosis. Blood lysyl oxidase (LOX), human epididymis protein 4 (HE4), and pentraxin-2 may potentially assess renal fibrosis, but are easily affected by other fibrotic diseases (liver fibrosis, pulmonary fibrosis, etc.) [28–30]. Non-invasive imaging examinations, such as B-ultrasound, indirectly reflect renal fibrosis through renal anatomical changes, making it difficult to determine the degree of renal fibrosis early and accurately. Due to the potential impact of contrast agents on renal function, enhanced CT is also unsuitable for evaluating renal fibrosis, especially

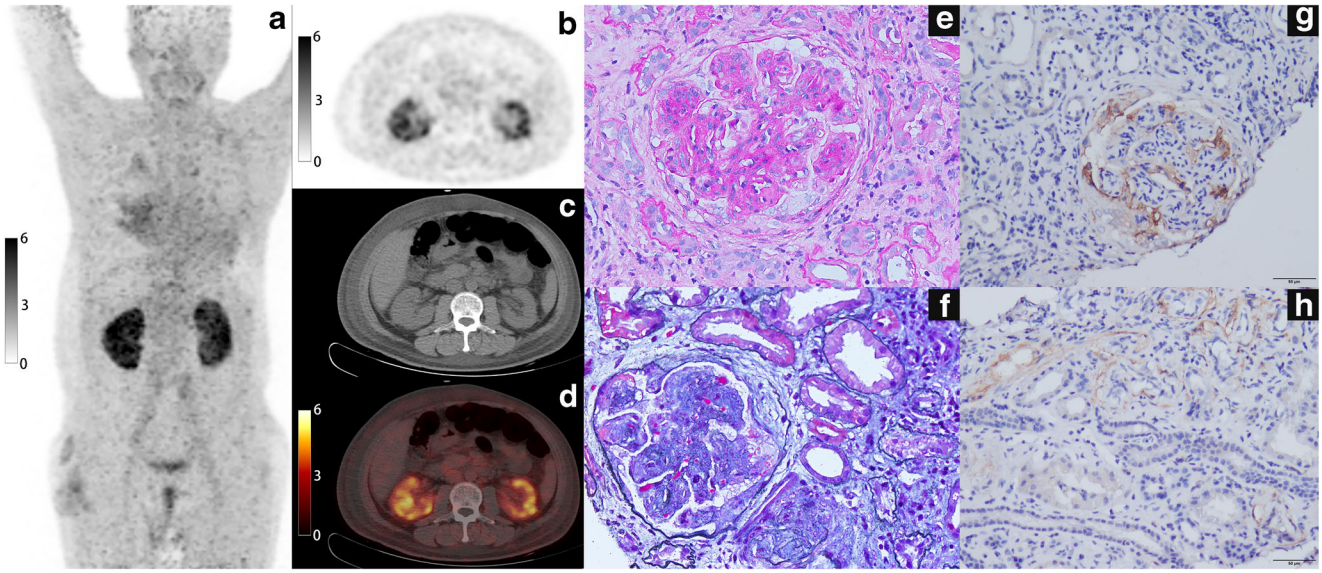

Fig. 1 A 58-year-old man experienced decreased urine output and proteinuria for 6 months and lower limb edema for 3 months. The maximum intensity projection (MIP) image of whole-body [^{68}Ga]Ga-FAPI-04 PET (**a**) shows diffuse uptake of radiotracer in both kidneys. The cross-sectional images (**b**–**d**) show moderate radiotracer uptake in both kidney parenchyma, and the SUVmax was 5.71, suggesting diffuse fibrosis of the kidneys. The pathological examination led to a diagnosis of membranoproliferative glomerulonephritis (severe renal interstitial fibrosis), which HE and PAS staining (**e**, **f**) supported. The immunochemical examination (**g**, **h**) found FAP in both the glomeruli and renal interstitium. The pathological results are consistent with the PET/CT examination results

for ESRD patients. The current imaging methods for assessing the degree of renal fibrosis are limited [31].

At present, kidney tissue biopsy is the main method of accurately assessing the presence and severity of renal fibrosis. Although reliable, it has some contraindications and may cause complications, which hinders its wide clinical application. It can only reflect fibrosis of the kidney tissue at the puncture site and not the overall degree of fibrosis [32].

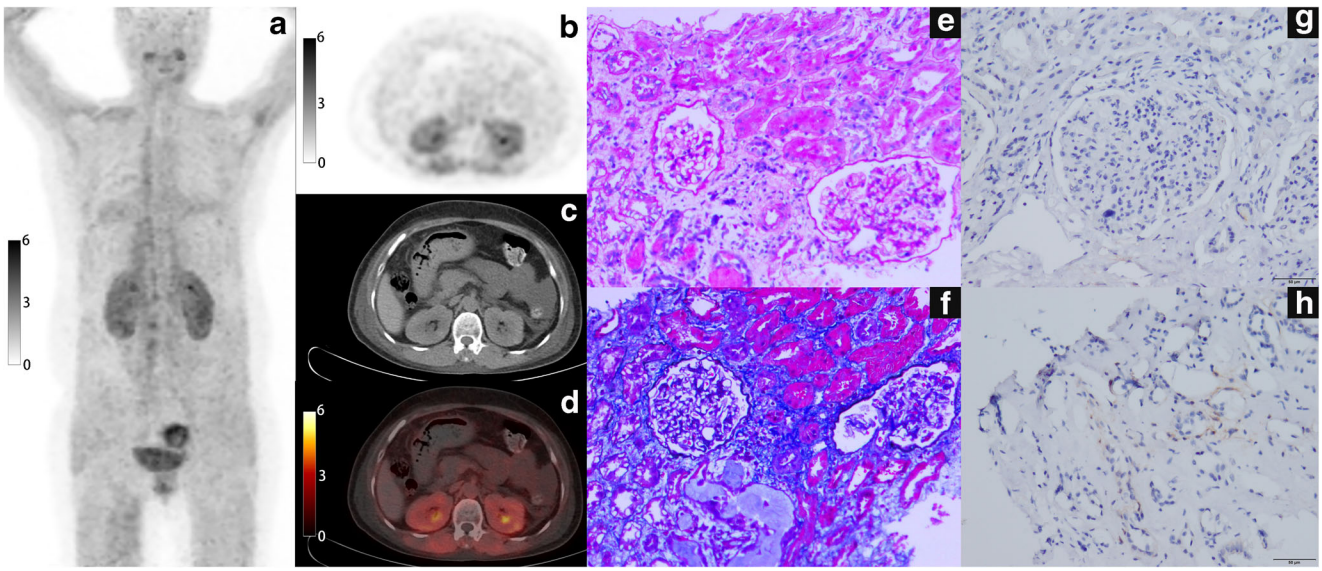

Fig. 2 A 56-year-old woman presented with edema and proteinuria with no obvious cause. The maximum intensity projection (MIP) image of whole-body [^{68}Ga]Ga-GAPI-04 PET (**a**) shows diffuse uptake of the radiotracer in both kidneys. The cross-sectional images (**b**–**d**) show that the kidney parenchyma had slight radiotracer uptake and the SUVmax was 4.4, suggesting diffuse fibrosis of both kidneys. The pathological examination led to a diagnosis of minimal change glomerulonephritis (mild fibrosis of renal interstitium). HE and PAS staining (**e**, **f**) supported this diagnosis. The immunochemical examination (**g**, **h**) found FAP in the renal interstitium, while no FAP was found in the globular tissue. The pathological results were consistent with the PET/CT results. In this case, the patient's bilateral erector spinae radiotracer uptake was slightly increased and the SUVmax was 3.0. Upon questioning, we found that the patient had a long-term occupational history of manual agriculture. The patient was diagnosed with erector spinae strain

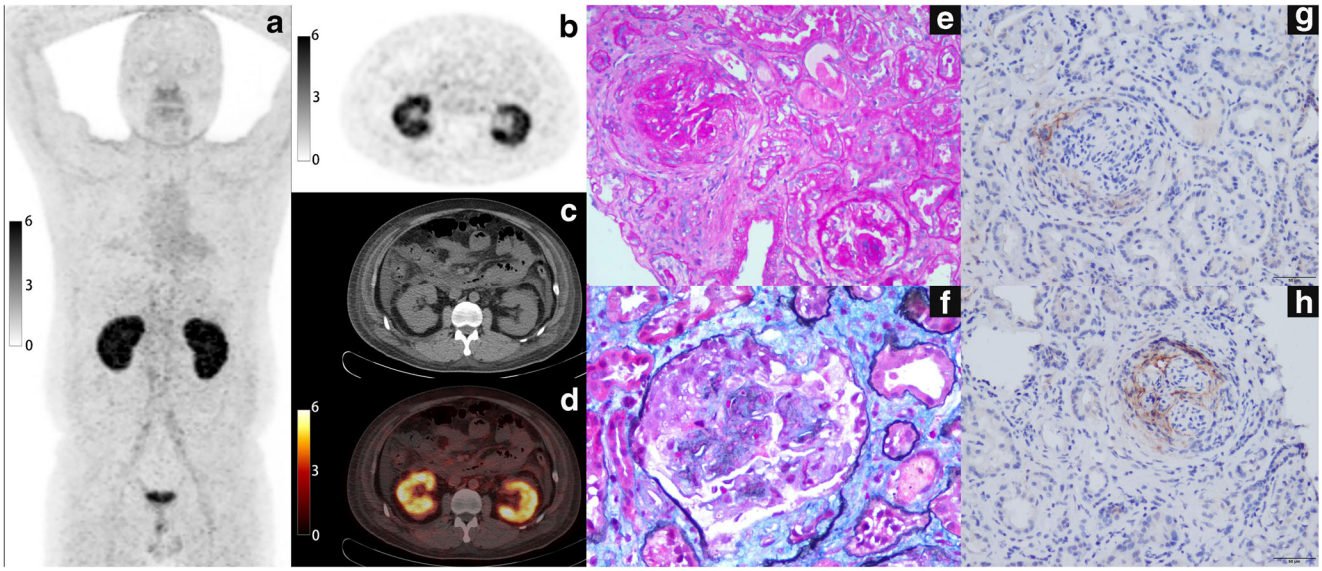

Fig. 3 A 30-year-old man presented with edema of his lower limbs and face for more than 4 months, with foamy urine and pleural effusion. The maximum intensity projection (MIP) image of whole-body [^{68}Ga]Ga-FAPI-04 PET (**a**) shows diffuse uptake of radiotracer in both kidneys. The cross-sectional images (**b**–**d**) show heavy radiotracer uptake in both kidney parenchyma, and the SUVmax was 7.3, suggesting diffuse fibrosis of the kidneys. The pathological examination led to a diagnosis of crescentic glomerulonephritis (glomerular and renal interstitial moderate fibrosis), and HE and PAS staining (**e**, **f**) supported this diagnosis. The immunochemical examination (**g**, **h**) found FAP in the glomerulus, but almost no FAP was found in the renal interstitium. The pathological results were consistent with the PET/CT results

Therefore, it is vital to find other non-invasive methods with better specificity and sensitivity to accurately assess the degree of renal fibrosis.

In this study, [^{68}Ga]Ga-FAPI-04 was used to detect renal fibrosis. It proved to be a promising new imaging method, with a higher uptake of radiotracer found in almost all patients (12/13). It was easier to distinguish the radiotracer with higher uptake of renal parenchyma from the background because of the high average values of TBR and SUVmax. We chose the liver as the background organ because the kidneys typically

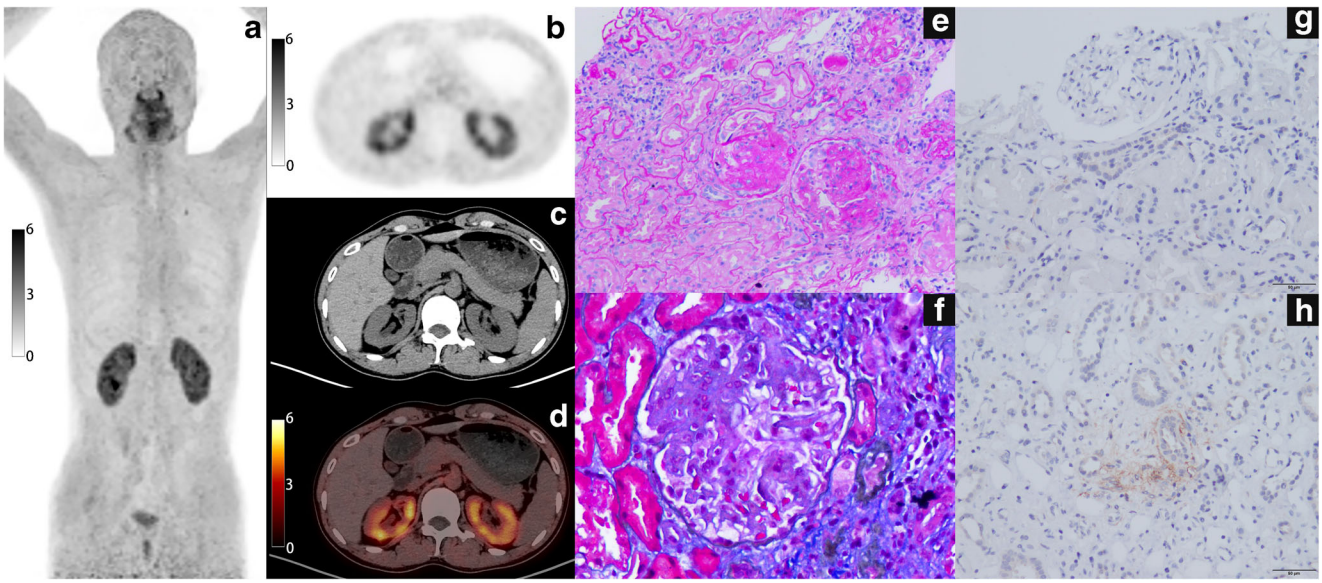

Fig. 4 A 25-year-old man had decreased renal function and proteinuria during a physical examination more than 3 months ago. The maximum intensity projection (MIP) image of whole-body [^{68}Ga]Ga-FAPI-04 PET (**a**) shows diffuse radiotracer uptake in both kidneys. The cross-sectional images (**b**–**d**) show light radiotracer uptake in both kidney parenchyma, and the SUVmax was 7.6, suggesting diffuse fibrosis of the kidneys. The pathological examination led to a diagnosis of mesangial proliferative glomerulonephritis (moderate fibrosis of glomerulus and renal interstitium). HE and PAS staining (**e**, **f**) supported this diagnosis. The immunochemical examination (**g**, **h**) found FAP in the renal interstitium. Almost no FAP was found in the glomerulus, which was consistent with the PET/CT results

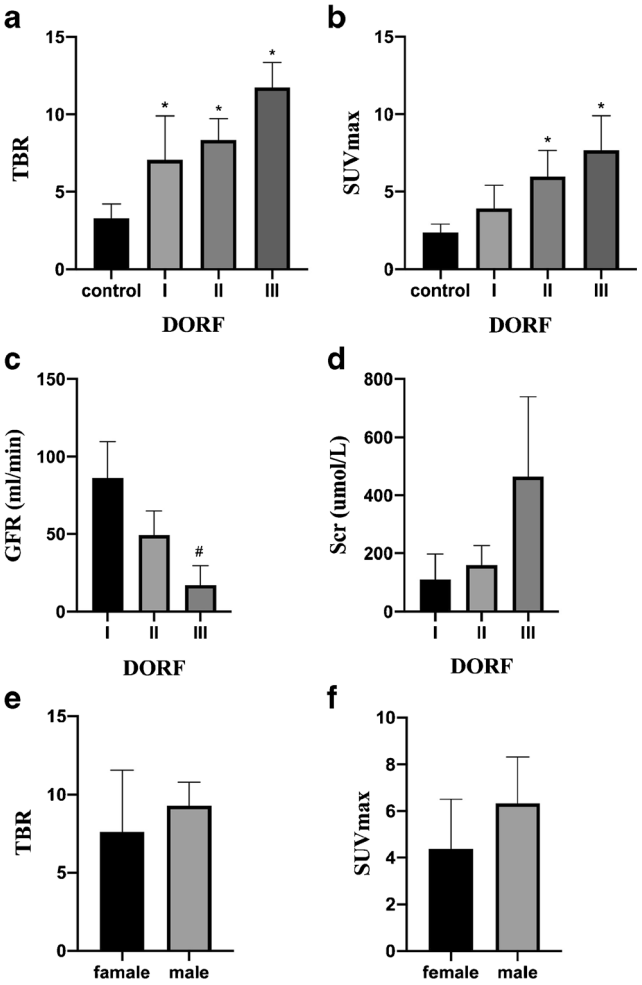

Fig. 5 A bar graph comparing the TBR (**a**), SUVmax (**b**), GFR (**c**), and Scr (**d**) of patients with different renal fibrosis grades and the TBR (**e**) and SUVmax (**f**) of patients by gender. The six sets of data revealed an obvious trend. A statistical significance of $P < 0.05$ was determined by the Kruskal-Wallis nonparametric rank-sum test (**a**, **b**, **c**, and **d**) and Mann-Whitney *U* test (**e** and **f**) (degree of renal fibrosis, DORF)

take up radiotracer diffusely, and it is difficult to choose normal kidney tissue as the background. Among the patients included in our study, a small number have specific uptake of radioactivity in the back muscles. In addition, patients with chronic kidney disease often suffer from protein loss from the whole body, leading to muscle edema and thinning. Therefore, we did not choose muscle tissue as the background. We did not select the skeletal system as the background as renal osteopathy causes bone changes.

In the included patients, liver uptake was uniform and was not affected by kidney disease, so we chose the liver as the background. The SUVmax and TBR of most patients correlated with the pathology of kidney tissue. [^{68}Ga]Ga-FAPIs PET/CT examination may enable diagnosis of renal fibrosis without a biopsy. Clinicians can instruct the kidney biopsy site for patients with focal renal fibrosis. [^{68}Ga]Ga-FAPIs PET/CT can also detect early renal fibrosis. Separate examinations before and after nephropathy treatment may also evaluate the effectiveness of clinical treatment methods.

This study has some limitations, including the fact that a small number of patients (2/13) had some residual radiotracer in the renal pelvis and calyces, which may have affected image quality. Also, the small number of study subjects and the unequal number of patients with various types of renal fibrosis limited the statistical significance. In the future, a larger patient cohort is needed to evaluate [^{68}Ga]Ga-FAPI PET/CT in renal fibrosis. In summary, compared with traditional renal puncture examinations, [^{68}Ga]Ga-FAPIs PET/CT can quickly show the histology of renal fibrosis. In patients for whom renal puncture is unsuitable, [^{68}Ga]Ga-FAPIs PET/CT scans can be used to determine rapid and effective treatment plans for improved results.

Research on [^{68}Ga]Ga-FAPIs in benign lesions has recently been progressing rapidly. Increased FAP has reportedly been found in refractory rheumatoid arthritis [33]. Besides renal fibrosis, high uptake of FAPI has been found in benign diseases such as liver fibrosis, arthritis, cardiovascular disease, Crohn's bowel disease, idiopathic retroperitoneal fibrosis, pancreatitis, and osteophytes [16, 34–40]. The diagnostic utility of [^{68}Ga]Ga-FAPIs requires further exploration.

Table 4 Control group data

Patient no.	Age/ gender	SUVmax of kidney	SUVmean of liver	TBR
1	50/F	2.3	1.42	2.911
2	49/M	2.29	1.68	3.94
3	44/M	3.4	1.304	3.73
4	27/M	2.006	1.013	2.48
5	54/M	1.62	1.23	2.07
6	43/M	2.75	0.822	4.66
7	25/F	2.5	1.797	2.52
8	28/M	2.6	0.761	4.41
9	58/F	1.725	1.005	2.97

Conclusion

The results of this preliminary study indicate that radiolabeled FAPI can be used to image renal fibrosis. The imaging quality of [^{68}Ga]Ga-FAPI-04 PET/CT scans in patients with moderate-to-severe renal fibrosis may be superior to other examination methods, but additional clinical trials are needed for further evaluation.

Declarations

Ethics approval and consent to participate All procedures involving human participants were performed in accordance with the ethical standards of the institutional committee, as well as the 1964 Helsinki Declaration and its later amendments or comparable ethical standards. This article does not contain any animal experiments.

Informed consent was obtained from all participants included in the study.

Consent for publication Informed consent was obtained from all participants included in the study.

Conflict of interest The authors declare no competing interests.

References

1. Majo J, Klinkhammer BM, Boor P, Tiniakos D. Pathology and natural history of organ fibrosis. Curr Opin Pharmacol. 2019;49:82–9. https://doi.org/10.1016/j.coph.2019.09.009.
2. Ruiz-Ortega M, Rayego-Mateos S, Lamas S, Ortiz A, Rodrigues-Diez RR. Targeting the progression of chronic kidney disease. Nat Rev Nephrol. 2020;16:269–88. https://doi.org/10.1038/s41581-019-0248-y.
3. Pyo JY, Ahn SS, Lee LE, Choe HN, Song JJ, Park YB, et al. Efficacy of the fibrosis index for predicting end-stage renal disease in patients with antineutrophil cytoplasmic antibody-associated vasculitis. Int J Clin Pract. 2020:e13929. https://doi.org/10.1111/ijcp.13929.
4. Zahir Z, Wani AS, Prasad N, Jain M. Clinicopathological characteristics and predictors of poor outcome in anti-glomerular basement membrane disease - a fifteen year single center experience. Ren Fail. 2021;43:79–89. https://doi.org/10.1080/0886022X.2020.1854301.
5. Zhang L, Wang F, Wang L, Wang W, Liu B, Liu J, et al. Prevalence of chronic kidney disease in China: a cross-sectional survey. Lancet. 2012;379:815–22. https://doi.org/10.1016/S0140-6736(12)60033-6.
6. Tang PM, Nikolic-Paterson DJ, Lan HY. Macrophages: versatile players in renal inflammation and fibrosis. Nat Rev Nephrol. 2019;15:144–58. https://doi.org/10.1038/s41581-019-0110-2.
7. Tang C, Livingston MJ, Liu Z, Dong Z. Autophagy in kidney homeostasis and disease. Nat Rev Nephrol. 2020;16:489–508. https://doi.org/10.1038/s41581-020-0309-2.
8. Tang S, Wang Y, Xie G, Li W, Chen Y, Liang J, et al. Regulation of Ptch1 by miR-342-5p and FoxO3 induced autophagy involved in renal fibrosis. Front Bioeng Biotechnol. 2020;8:583318. https://doi.org/10.3389/fbioe.2020.583318.
9. Eddy AA. Overview of the cellular and molecular basis of kidney fibrosis. Kidney Int Suppl (2011). 2014;4:2–8. https://doi.org/10.1038/kisup.2014.2.
10. Lipphardt M, Dihazi H, Jeon NL, Dadafarin S, Ratliff BB, Rowe DW, et al. Dickkopf-3 in aberrant endothelial secretome triggers renal fibroblast activation and endothelial-mesenchymal transition. Nephrol Dial Transplant. 2019;34:49–62. https://doi.org/10.1093/ndt/gfy100.
11. Yuan Q, Tan RJ, Liu Y. Myofibroblast in kidney fibrosis: origin, activation, and regulation. Adv Exp Med Biol. 2019;1165:253–83. https://doi.org/10.1007/978-981-13-8871-2_12.
12. Acharya PS, Zukas A, Chandan V, Katzenstein AL, Pure E. Fibroblast activation protein: a serine protease expressed at the remodeling interface in idiopathic pulmonary fibrosis. Hum Pathol. 2006;37:352–60. https://doi.org/10.1016/j.humpath.2005.11.020.
13. Luo Y, Pan Q, Zhang W. IgG4-related disease revealed by ^{68}Ga-FAPI and 18F-FDG PET/CT. Eur J Nucl Med Mol Imaging. 2019;46:2625–6. https://doi.org/10.1007/s00259-019-04478-2.
14. Hao B, Wu X, Pang Y, Sun L, Wu H, Huang W, et al. [(18)F]FDG and ([68)Ga]Ga-DOTA-FAPI-04 PET/CT in the evaluation of tuberculous lesions. Eur J Nucl Med Mol Imaging. 2021;48:651–2. https://doi.org/10.1007/s00259-020-04941-5.
15. Chen H, Pang Y, Wu J, Zhao L, Hao B, Wu J, et al. Comparison of [$^{(68)}$Ga]Ga-DOTA-FAPI-04 and [(18)F] FDG PET/CT for the diagnosis of primary and metastatic lesions in patients with various types of cancer. Eur J Nucl Med Mol Imaging. 2020;47:1820–32. https://doi.org/10.1007/s00259-020-04769-z.
16. Luo Y, Pan Q, Zhang W, Li F. Intense FAPI uptake in inflammation may mask the tumor activity of pancreatic cancer in ^{68}Ga-FAPI PET/CT. Clin Nucl Med. 2020;45:310–1. https://doi.org/10.1097/RLU.0000000000002914.
17. Wynn TA. Cellular and molecular mechanisms of fibrosis. J Pathol. 2008;214:199–210. https://doi.org/10.1002/path.2277.
18. Liu Y. Cellular and molecular mechanisms of renal fibrosis. Nat Rev Nephrol. 2011;7:684–96. https://doi.org/10.1038/nrneph.2011.149.
19. Conway B, Hughes J. Cellular orchestrators of renal fibrosis. QJM. 2012;105:611–5. https://doi.org/10.1093/qjmed/hcr235.
20. Liu Y. Renal fibrosis: new insights into the pathogenesis and therapeutics. Kidney Int. 2006;69:213–7. https://doi.org/10.1038/sj.ki.5000054.
21. Nakaigawa N, Kondo K, Kaneta T, Tateishi U, Minamimoto R, Namura K, et al. FDG PET/CT after first molecular targeted therapy predicts survival of patients with renal cell carcinoma. Cancer Chemother Pharmacol. 2018;81:739–44. https://doi.org/10.1007/s00280-018-3542-7.
22. Sonni I, Lee-Felker S, Memarzadeh S, Quinn MM, Mona CE, Luckerath K, et al. $^{(68)}$Ga-FAPi-46 diffuse bilateral breast uptake in a patient with cervical cancer after hormonal stimulation. Eur J Nucl Med Mol Imaging. 2020. https://doi.org/10.1007/s00259-020-04947-z.
23. Wang L, Zhang Z, Zhao Z, Yan C, Fang W. $^{(68)}$Ga-FAPI right heart uptake in a patient with idiopathic pulmonary arterial hypertension. J Nucl Cardiol. 2020. https://doi.org/10.1007/s12350-020-02407-7.
24. Jiang K, Ferguson CM, Lerman LO. Noninvasive assessment of renal fibrosis by magnetic resonance imaging and ultrasound techniques. Transl Res. 2019;209:105–20. https://doi.org/10.1016/j.trsl.2019.02.009.
25. Gao J, Rubin JM, Weitzel W, Lee J, Dadhania D, Kapur S, et al. Comparison of ultrasound corticomedullary strain with Doppler parameters in assessment of renal allograft interstitial fibrosis/tubular atrophy. Ultrasound Med Biol. 2015;41:2631–9. https://doi.org/10.1016/j.ultrasmedbio.2015.06.009.

26. O'Neill WC. Sonographic evaluation of renal failure. Am J Kidney Dis. 2000;35:1021–38. https://doi.org/10.1016/s0272-6386(00)70036-9.
27. Nijssen EC, Rennenberg R, Nelemans P, van Ommen V, Wildberger JE. Post-contrast acute kidney injury and intravenous prophylactic hydration: an update. Rofo. 2021;193:151–9. https://doi.org/10.1055/a-1248-9178.
28. Zhang XQ, Li X, Zhou WQ, Liu X, Huang JL, Zhang YY, et al. Serum Lysyl oxidase is a potential diagnostic biomarker for kidney fibrosis. Am J Nephrol. 2020;51:907–18. https://doi.org/10.1159/000509381.
29. Basturk T, Ojalvo D, Mazi EE, Hasbal NB, Ozagari AA, Ahbap E, et al. Pentraxin-2 is associated with renal fibrosis in patients undergoing renal biopsy. Clinics (Sao Paulo). 2020;75:e1809. https://doi.org/10.6061/clinics/2020/e1809.
30. Chen P, Yang Q, Li X, Qin Y. Potential association between elevated serum human epididymis protein 4 and renal fibrosis: a systemic review and meta-analysis. Medicine (Baltimore). 2017;96:e7824. https://doi.org/10.1097/MD.0000000000007824.
31. Nijssen EC, Rennenberg R, Nelemans P, van Ommen V, Wildberger JE. Post-contrast acute kidney injury and intravenous prophylactic hydration: an update. Rofo. 2020. https://doi.org/10.1055/a-1248-9178.
32. Luciano RL, Moeckel GW. Update on the native kidney biopsy: core curriculum 2019. Am J Kidney Dis. 2019;73:404–15. https://doi.org/10.1053/j.ajkd.2018.10.011.
33. Bauer S, Jendro MC, Wadle A, Kleber S, Stenner F, Dinser R, et al. Fibroblast activation protein is expressed by rheumatoid myofibroblast-like synoviocytes. Arthritis Res Ther. 2006;8:R171. https://doi.org/10.1186/ar2080.
34. Xu T, Zhao Y, Ding H, Cai L, Zhou Z, Song Z, et al. [$^{(68)}$Ga]Ga-DOTA-FAPI-04 PET/CT imaging in a case of prostate cancer with shoulder arthritis. Eur J Nucl Med Mol Imaging. 2020. https://doi.org/10.1007/s00259-020-05028-x.
35. Liu H, Wang Y, Zhang W, Cai L, Chen Y. Elevated [$^{(68)}$Ga]Ga-DOTA-FAPI-04 activity in degenerative osteophyte in a patient with lung cancer. Eur J Nucl Med Mol Imaging. 2020. https://doi.org/10.1007/s00259-020-05090-5.
36. Luo Y, Pan Q, Xu H, Zhang R, Li J, Li F. Active uptake of $^{(68)}$Ga-FAPI in Crohn's disease but not in ulcerative colitis. Eur J Nucl Med Mol Imaging. 2020. https://doi.org/10.1007/s00259-020-05129-7.
37. Zhao L, Gu J, Fu K, Lin Q, Chen H. ^{68}Ga-FAPI PET/CT in assessment of liver nodules in a cirrhotic patient. Clin Nucl Med. 2020;45:e430–e2. https://doi.org/10.1097/RLU.0000000000003015.
38. Heckmann MB, Reinhardt F, Finke D, Katus HA, Haberkorn U, Leuschner F, et al. Relationship between cardiac fibroblast activation protein activity by positron emission tomography and cardiovascular disease. Circ Cardiovasc Imaging. 2020;13:e010628. https://doi.org/10.1161/CIRCIMAGING.120.010628.
39. Hao B, Wu X, Pang Y, Sun L, Wu H, Huang W, et al. [$^{(18)}$F]FDG and [$^{(68)}$Ga]Ga-DOTA-FAPI-04 PET/CT in the evaluation of tuberculous lesions. Eur J Nucl Med Mol Imaging. 2020. https://doi.org/10.1007/s00259-020-04941-5.
40. Schmidkonz C, Rauber S, Atzinger A, Agarwal R, Gotz TI, Soare A, et al. Disentangling inflammatory from fibrotic disease activity by fibroblast activation protein imaging. Ann Rheum Dis. 2020;79:1485–91. https://doi.org/10.1136/annrheumdis-2020-217408.